Supporting Information

A pH-triggered fluorescence-switchable extracellular vesicle for tracing drug release and improving drug delivery

Rui Su, Xiang Xiong, Yingping Li, Xiaoqing Wei, Sibo Zheng, Jingya Zhao*, Shaobing Zhou*

Key Laboratory of Advanced Technologies of Materials, Ministry of Education, School of Materials Science and Engineering, Southwest Jiaotong University, Chengdu 610031, China.

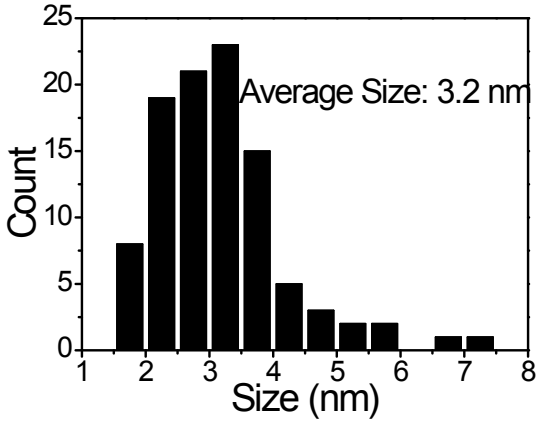

Fig. S1. Particle size distribution of the CDs analyzed from the TEM image (determined by randomly counting 100 particles).

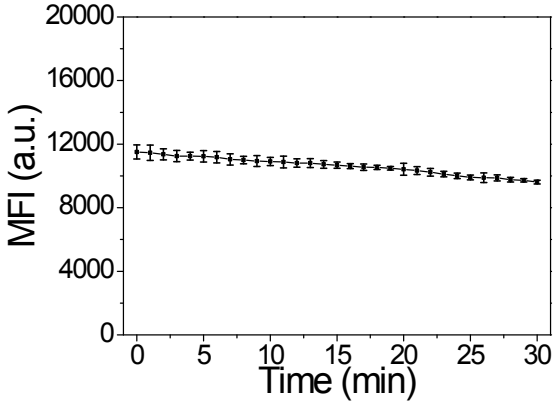

Fig. S2. Fluorescence intensity of CDs under continuous illumination for 30 min. The mean fluorescence intensity was acquired by calculation of the fluorescence images obtained from a fluorescence microscope. All statistical data are presented as mean ± standard deviation (n = 3; *p < 0.05, **p < 0.01, ***p < 0.001).

Table S1. The loading content and encapsulation efficiency for DOX and CDs.

	LC (%)	EE (%)
DOX	14.1%	57.8%
CDs	8.9%	48.6%

The loading content and encapsulation efficiency for DOX and CDs were supplemented and added to the revised supporting information as Table S1. The loading content (LC) is calculated using the Equation 1, and the loading efficiency (EE) is calculated by following Equation 2. X is DOX or CDs.

$$LC\ (\%) = \frac{Weight\ of\ X\ loaded\ in\ MVs@CDs - DOX}{Weight\ of\ MVs@CDs - DOX} \times 100\%$$

(1)

$$EE\ (\%) = \frac{Weight\ of\ X\ loaded\ in\ MVs@CDs - DOX}{Weight\ of\ X\ in\ feed} \times 100\%$$

(2)

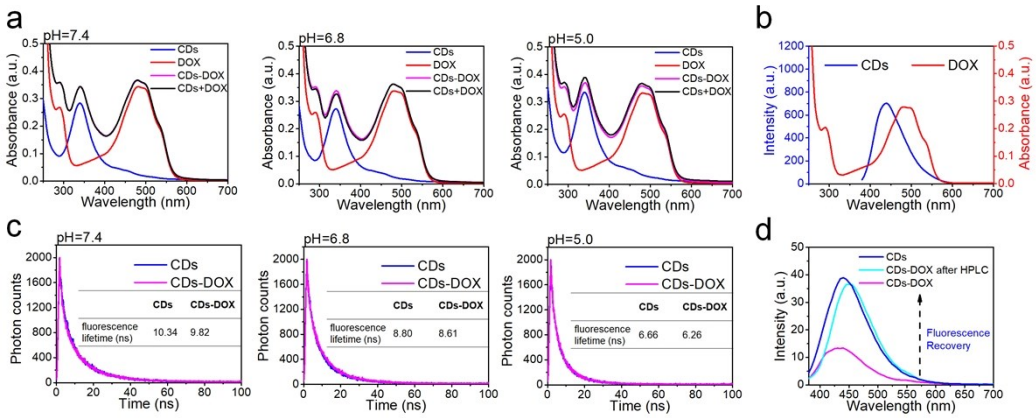

Fig. S3. Investigation of fluorescence quenching mechanism. a) UV−Vis absorption of CDs, DOX, CDs-DOX, and CDs+DOX (the sum of the CDs and DOX) at different pH. b) UV−Vis absorption of DOX and fluorescence spectra (excited at 360 nm) of CDs. c) The fluorescence decay curves and the fluorescence decay time of CDs and CDs-DOX at different pH (Ex: 360 nm). d) Fluorescence spectra of CDs without or with DOX, and CDs-DOX after separated from DOX (Ex: 360 nm).

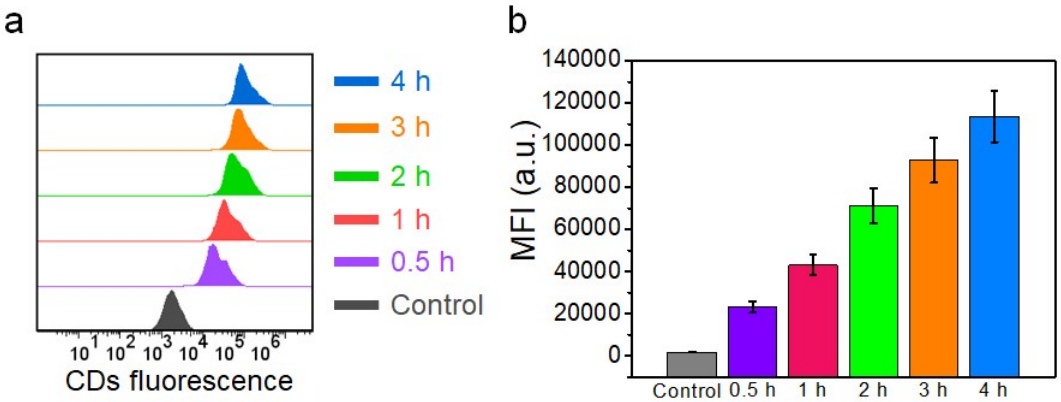

Fig. S4. Flow cytometry analysis in cellular uptake. a) The uptake of MVs@CDs by 4T1 cells with 0.5 h, 1 h, 2 h, 3 h, and 4 h. b) Mean fluorescence intensity of different time points. All statistical data are presented as mean ± standard deviation (n = 3; *p < 0.05, **p < 0.01, ***p < 0.001)

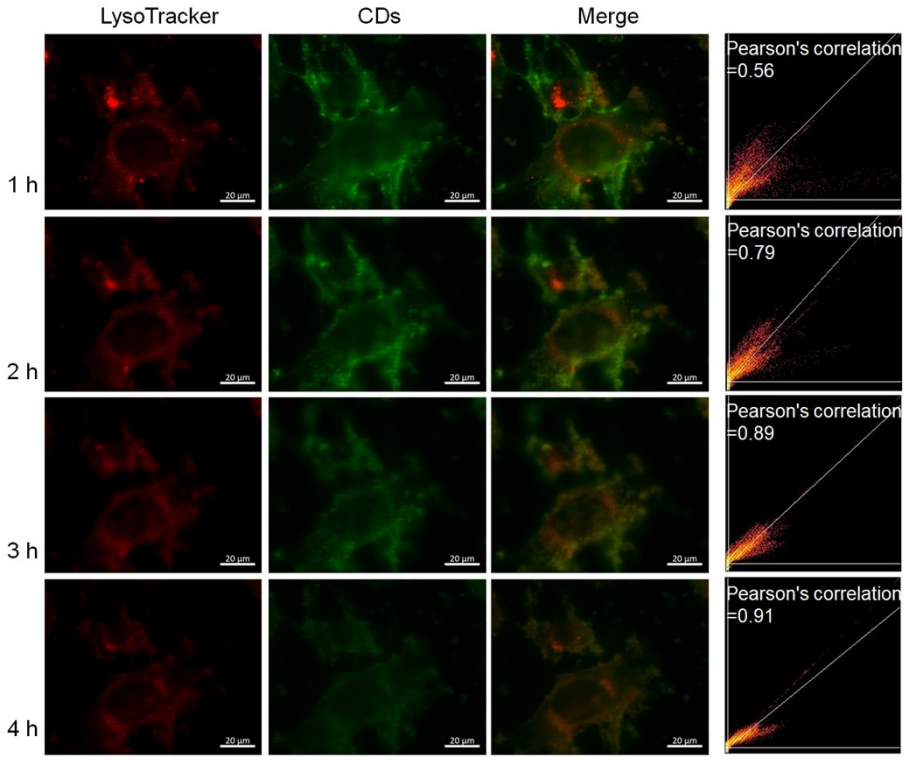

Fig. S5. Co-localization of lysosomes and MVs@CDs in 4T1 cells images and scatter plot of correalation coefficient.

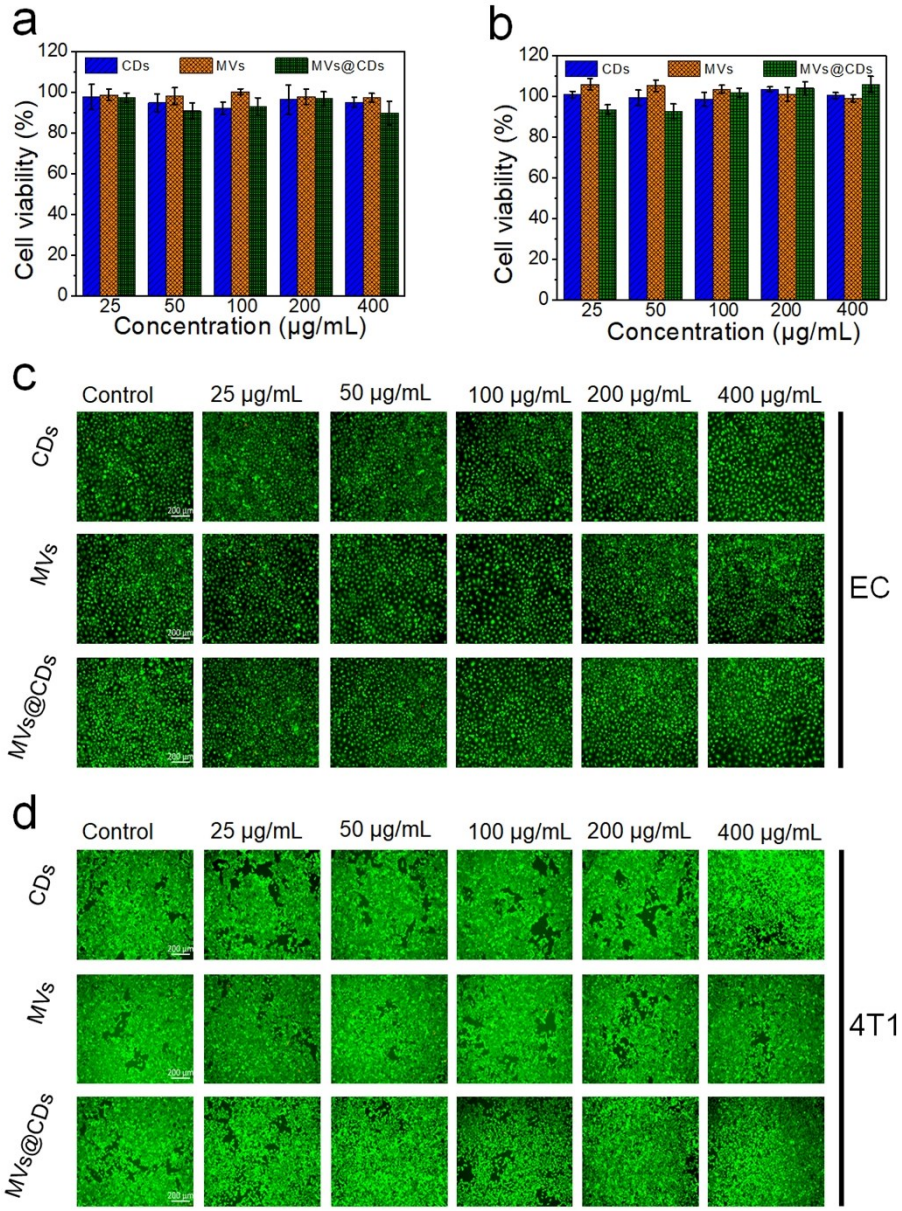

Fig. S6. Cytocompatibility evaluation. a) Cell viabilities of EC cells treated with CDs, MVs or MVs@CDs of different concentrations. b) Corresponding fluorescence images showing the viability of EC cells. c) Cell viabilities of 4T1 cells treated with CDs, MVs or MVs@CDs of different concentrations. d) Corresponding fluorescence images showing the viability of 4T1 cells. All statistical data are presented as mean ± standard deviation (n = 3; *p < 0.05, **p < 0.01, ***p < 0.001).

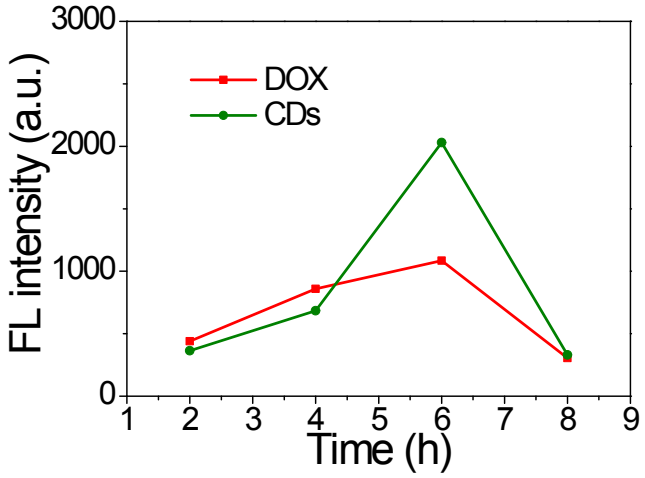

Fig. S7. Statistical mean fluorescence intensity of tumor tissue sections at 2, 4, 6, and 8 h after intratumoral injection of MVs@CDs-DOX.